Inorg. Chem. **2004**, *43*, 3673–3681

Electrochemical, Spectroscopic, and Structural Evidence for the Mild Hydrolysis of Tetracyanoethylene, TCNE, To Form the 2,3,3-Tricyanoacrylamidate Ligand: Isolation of an Unexpected Quadruply-Bonded Polymeric Material $[Mo_2(O_2CCMe_3)_3((NC)_2CC(CN)CONH)]_\infty$

Françoise Conan,[†] Benoît Le Gall,[†] Jean-Michel Kerbaol,[†] Sylvie Le Stang,[†] Jean Sala-Pala,[†] Yves Le Mest,*[,†] John Bacsa,[‡] Xiang Ouyang,[‡] Kim R. Dunbar,*[,‡] and Charles F. Campana[§]

Laboratoire de Chimie, Electrochimie Moléculaires et Chimie Analytique, UMR CNRS 6521, Université de Bretagne Occidentale, CS 93837, 6 av. Victor Le Gorgeu, 29238 Brest Cedex 3, France, Department of Chemistry, Texas A&M University, College Station, Texas 77842-3012, and Bruker AXS Inc., 5465 East Cheryl Parkway, Madison, Wisconsin 53711-5373

Received September 23, 2003

Under strictly anhydrous conditions, no reaction occurs between $Mo_2(O_2CCMe_3)_4$ and tetracyanoethylene, TCNE, at room temperature, but after addition of 1 equiv of water, a reaction proceeds to form $[Mo_2(O_2CCMe_3)_3((NC)_2CC(CN)CONH)]$, **1**. The compound contains a quadruple-bonded Mo_2 unit and the 2,3,3-tricyanoacrylamidate anion as a ligand (TC3A), a very unusual hydrolyzed form of TCNE. Two different solid-state structures were obtained after crystallization of **1**. Crystals obtained from CH_2Cl_2 consist of a two-dimensional network, and crystals grown from a C_6H_6 solution form a 1-D chain motif. In both cases, the TC3A ligand acts as a polydentate ligand involving a bidentate OCN bridging unit and two CN groups. The electrochemical and spectroscopic (IR, UV/vis/near-IR, NMR, EPR) properties of **1** support the formulation in solution as a discrete 1:1 complex of the TC3A donor ligand and a Mo_2 unit with no charge transfer. The coordinated TC3A ligand exhibits redox properties similar to those of free TCNE.

Introduction

The charge-transfer reactions of inorganic donors with organic acceptors of the TCNX family (TCNE = tetracyanoethene, TCNQ = 7,7,8,8-tetracyano-*p*-quinodimethane) continues to receive considerable attention in the field of molecular materials,[1−3] owing to the variable redox states (0, •−, 2−) and binding modes [σ-η^1(N) or π-η^2(C=C)] of these molecules.[2] An area of particular interest is the reactivity of TCNX derivatives with electron-rich metal complexes to form discrete as well as polymeric charge-transfer compounds in which the donors and acceptors are coordinated through nitrile positions.[3−7] Among the systems that we and others have been investigating in this general area are metal−metal bonded species,[4,5,8,9] efforts that include the chemistry of tetracarboxylate compounds $Mo_2(O_2CR)_4$ (R = Me, CMe_3, $CH_2CH_2CHMe_2$, CF_3) with polycyano acceptor ligands.

Herein, we describe an unusual reaction between $Mo_2(O_2CCMe_3)_4$ and TCNE. While no reaction was observed to occur under strictly anhydrous conditions, the addition of 1 equiv of water leads to the formation of $[Mo_2(O_2CCMe_3)_3((NC)_2CC(CN)CONH)]$, **1**, which contains a Mo-4-Mo unit and the unusual hydrolyzed form of the TCNE ligand, 2,3,3-tricyanoacrylamidate anion (TC3A). The electrochemical and spectroscopic (IR, UV/vis/near-IR, NMR, EPR) properties of **1** support the formulation in solution as a discrete 1/1

* To whom correspondence should be addressed. Y.L.M.: e-mail, yves.lemest@univ-brest.fr; fax, +33-2-98017001. K.R.D.: e-mail, dunbar@mail.chem.tamu.edu; fax, + 01-(979)-845-7177.
† Université de Bretagne Occidentale.
‡ Texas A&M University.
§ Bruker AXS Inc.

(1) (a) Miller, J. S. *Inorg. Chem.* **2000**, *39*, 4392. (b) Hibbs, W.; Rittenberg, D. K.; Sugiura, K.-I.; Burkhart, B. M.; Morin, B. G.; Arif, A. M.; Liable-Sands, L.; Rheingold, A. L.; Sundaralingam, M.; Epstein, A. J.; Miller, J. S. *Inorg. Chem.* **2001**, *40*, 1915.
(2) (a) Kaim, W.; Moscherosch, M. *Coord. Chem. Rev.* **1994**, *129*, 157. (b) Dunbar, K. R. *Angew. Chem., Int. Ed. Engl.* **1996**, *35*, 1659.

10.1021/ic0351186 CCC: $27.50
Published on Web 05/15/2004

complex of the TC3A ligand and a [Mo-4-Mo] moiety. Two different solid-state structures of compound **1** were obtained from CH_2Cl_2 and benzene, namely, a two-dimensional motif and a 1-D chain, respectively. The coordinated TC3A ligand exhibits redox properties similar to those of TCNE, namely, it is reduced in two one-electron steps, which indicates that charge transfer has not occurred between the metal−metal bonded donor and the organic acceptor in spite of their well-matched redox potentials. To our knowledge, this is the first example of an "innocent" adduct of an acceptor and a multiply bonded dimetal unit donor.[3−5]

Experimental Section

Materials and Methods. All reactions were performed in Schlenk tubes in a dry dinitrogen atmosphere. Solvents were distilled using standard techniques and were thoroughly deoxygenated before use. Samples for physical measurements were prepared inside a drybox (Jacomex). IR spectra were obtained with the use of a Nicolet Nexus spectrometer (KBr pellets or CH_2Cl_2 solution). ^{1}H and ^{13}C NMR spectra were recorded on a Bruker AMX 400 MHz. EPR spectra were recorded using a Bruker Elexys spectrometer (X-band). The UV/vis/near-IR spectrophotometer that was used is a Hitachi U-2010. The high-resolution mass spectrometry data were recorded on a ZabSpec TOF Micromass at CRMPO (Université de Rennes 1). The recording conditions were positive LSIMS (Cs^+), 8 kV acceleration, temperature 40 °C, matrix mNBA. Elemental analyses were performed by the "Service Central d'Analyses du CNRS", Vernaison, France. The starting material $Mo_2(O_2CCMe_3)_4$ was prepared as described in the literature.[10] The TCNE reagent was purchased from Aldrich. All electrochemical experiments were carried out in a dry oxygen free atmosphere (N_2) box. The electrochemical cell was specifically designed to fit the rotating disk electrode (EDI Tacussel) for a minimum volume of solution in the main compartment. The auxiliary and reference (ferrocenium/ferrocene = Fc^+/Fc) electrodes were in separate compartments connected to the main one through ground joints terminated by frits (Vycor tips from PAR). For voltammetric measurements, a platinum disk (∅ = 2 mm) was employed, and the electrolyses were performed with the same electrode, but rotated and equipped with a 4 mm diameter disk. A model PAR 173 potentiostat equipped with a PAR 179 digital coulometric unit and a T-2Y SEFRAM Enertec chart recorder was monitored by a PAR 175 programmer.

Syntheses. $[Mo_2(O_2CCMe_3)_3\{(NC)_2CC(CN)CONH\}]$, 1. After addition of TCNE (0.064 g, 0.5 mmol) in acetonitrile (ca. 30 mL) to $Mo_2(O_2CCMe_3)_4$ (0.300 g, 0.5 mmol), the mixture was stirred at ambient temperature for 1.5 h. In the presence of water, residual or deliberately added (vide infra), the solution color rapidly turned from bright yellow to deep green. The volatile materials were then removed under reduced pressure, and the residue was extracted with ca. 20 mL of dichloromethane, filtered and left at −20 °C for several days. Dichroic green-red hexagonal crystals were collected. Yield after crystallization: 47%. Apparently facile loss of interstitial solvent molecules rendered it difficult to analyze single crystals despite many determined attempts; therefore the elemental analysis was measured on a powder after pumping in vacuo for ca. 12 h. Calcd for $C_{21}H_{28}Mo_2N_4O_7$: C 39.4, H 4.4, N 8.8. Found: C 39.6, H 4.5, N 8.6. IR (KBr): $\bar{\nu}$ = 3359w, 3336w (ν(NH)), 2200s, 2179m, 2158w, 2149w (ν(CN)), 1430−1360w cm^{-1} (ν(CO)). IR (CH_2Cl_2): $\bar{\nu}$ = 2204s, 2219sh cm^{-1} (ν(CN)). ^{1}H NMR (CD_3CN): δ = 1.40 (s, 9 H, CH_3), 1.45 (s, 18 H, CH_3); 11.75 (s broad, 1H, OH). ^{13}C NMR (CD_3CN): δ = 28.3, 28.4 (C(CH_3)$_3$), 41.7, 41.8 (C(CH_3)$_3$), 83.7, 105.1, 111.1, 111.9, 114.3, 164.3 (CN, $C{=}C$), 195.9, 197.2 (OCO). MS: calcd for $C_{21}H_{28}N_4O_7{}^{92}Mo^{98}Mo$, 638.0080; found, 637.9962.

The same reaction was noted to occur in slightly wet CH_2Cl_2.[11]

Single-Crystal X-ray Studies and Crystal Growth. $\{[Mo_2(O_2CCMe_3)_3((NC)_2CC(CN)CONH)]\cdot 10CH_2Cl_2\}_\infty$, 2. A dark brown CH_2Cl_2 solution of **1** was placed in a programmable Cryogen II-80 low-temperature bath. The temperature was set to circulate between −10 and −40 °C with a gradient of +1 °C/h. After ∼ 1 week, red hexagonal-shaped crystals in the size range of 0.2−0.4 mm diameter were obtained. Within 2 weeks, the crystals were in the millimeter size range.

$\{[Mo_2(O_2CCMe_3)_3((NC)_2CC(CN)CONH)]\cdot C_6H_6\}_\infty$, 3. A CH_2Cl_2 solution of **1** was stored in a low-temperature bath (∼−20 °C), and the solvent was removed by a dynamic vacuum. Freshly distilled benzene was added to the resulting residue, and the dark green solution was transferred to a Schlenk flask by a cannula. The solution was stored at room temperature for 1 week, during which time dark red hexagonal platelet crystals formed.

Data Collection. $\{[Mo_2(O_2CCMe_3)_3((NC)_2CC(CN)CONH)]\cdot 10CH_2Cl_2\}_\infty$, 2. A red hexagonal-shaped specimen of approximate dimensions 0.46 × 0.40 × 0.20 mm^3 was selected for X-ray crystallographic analysis. The selected crystal was coated with a cryoprotectant consisting of a mixture of dichloromethane and

(3) (a) Clérac, R.; O'Kane, S.; Cowen, J.; Ouyang, X.; Heintz, R. A.; Zhao, H.; Dunbar, K. R. *Chem. Mater*. **2003**, *15*, 1840. (b) O'Kane, S. A.; Clérac, R.; Zhao, H.; Ouyang, X.; Galan-Mascaros, J. R.; Heintz, R.; Dunbar, K. R. *J. Solid State Chem.* **2000**, *152*, 159. (c) Heintz, R. A.; Zhao, H.; Ouyang, X.; Grandinetti, G.; Cowen, J.; Dunbar, K. R. *Inorg. Chem.* **1999**, *38*, 144. (d) Ballester, L.; Gutiérrez, A.; Perpinan, M. F.; Azcondo, M. T. *Coord. Chem. Rev.* **1999**, *190*−*192*, 447. (e) Zhao, H.; Heintz, R. A.; Ouyang, X.; Dunbar, K. R.; Campana, C. F.; Rogers, R. D. *Chem. Mater*. **1999**, *11*, 736. (f) Ballester, L.; Gutiérrez, A.; Perpinan, M. F.; Amador, U.; Azcondo, M. T.; Sanchez, A. E.; Bellito, C. *Inorg. Chem.* **1997**, *36*, 6390. (g) Ballester, L.; Gil, A. M.; Gutiérrez, A.; Perpinan, M. F.; Azcondo, M. T.; Sanchez, A. E.; Amador, U.; Campo, J.; Palacio, F. *Inorg. Chem.* **1997**, *36*, 5291. (h) Zhao, H.; Heintz, R. A.; Dunbar, K. R.; Rogers, R. *J. Am. Chem. Soc*. **1996**, *118*, 12844. (i) Kunkeler, P. J.; van Koningsbruggen, P. J.; Cornelissen, J. P.; van der Horst, A. N.; van der Kraan, A. M.; Spek, A. L.; Haasnoot, J. G.; Reedijk, J. *J. Am. Chem. Soc*. **1996**, *118*, 2190. (j) Cornelissen, J. P.; van Diemen, J. H.; Groeneveld, L. R.; Haasnoot, J. G.; Spek, A. L.; Reedijk, J. *Inorg. Chem*. **1992**, *31*, 198. (k) Ballester, L.; Barral, M. C.; Gutiérrez, A.; Jiménez-Aparicio, R.; Martinez-Muyo, J. M.; Perpiñan, M. F.; Monge, M. A.; Ruiz-Valero, C. *J. Chem. Soc., Chem. Commun*. **1991**, 1396. (l) Lacroix, L.; Kahn, O.; Gleizes, A.; Valade, L.; Cassoux, P. *Nouv. J. Chim.* **1985**, 643. (m) Shields, L. *J. Chem. Soc., Faraday Trans. 2* **1985**, *81*, 1.

(4) (a) Bartley, S. L.; Dunbar, K. R. *Angew. Chem., Int. Ed. Engl*. **1991**, *30*, 448. (b) Miyasaka, H.; Campos-Fernandez, C. S.; Clérac, R.; Dunbar, K. R. *Angew. Chem., Int. Ed.* **2000**, *39*, 3831. (c) Campana, C.; Dunbar, K. R.; Ouyang, X. *Chem. Commun.* **1996**, 2427. (d) Cotton, F. A.; Kim, Y.; Lu, J. *Inorg. Chim. Acta* **1994**, *221*, 1. (e) Dunbar, K. R. *J. Cluster Sci*. **1994**, *5*, 125. (f) Cotton, F. A.; Kim, Y. *J. Am. Chem. Soc.* **1993**, *115*, 8511. (g) Wesemann, J. L.; Chisholm, M. H. *Inorg. Chem*. **1997**, *36*, 3258.

(5) Dunbar, K. R.; Ouyang, X. *Mol. Cryst. Liq. Cryst. Sci. Technol., Sect. A* **1995**, *273*, 459.

(6) Bell, S. E.; Field, J. S.; Haines, R. J.; Moscherosch, M.; Matheis, W.; Kaim, W. *Inorg. Chem.* **1992**, *31*, 3269.

(7) Hartmann, H.; Kaim, W.; Hartenbach, I.; Schleid, T.; Wanner, M.; Fiedler, J. *Angew. Chem., Int. Ed.* **2001**, *40*, 2842.

(8) Kerbaol, J.-M.; Furet, E.; Guerchais, J. E.; Le Mest, Y.; Saillard, J.-Y.; Sala-Pala, J.; Toupet, L. *Inorg. Chem.* **1993**, *32*, 713.

(9) Giraudon, J.-M.; Guerchais, J. E.; Sala-Pala, J.; Toupet, L. *J. Chem. Soc., Chem. Commun.* **1988**, 921.

(10) McCarley, R. E.; Templeton, J. L.; Colburn, T. J.; Katovic, V.; Hoxmeier, R. J. *Adv. Chem. Ser*. **1976**, *150*, 318.

(11) Ouyang, X. Thesis, Texas A&M University, College Station, TX, 1999.

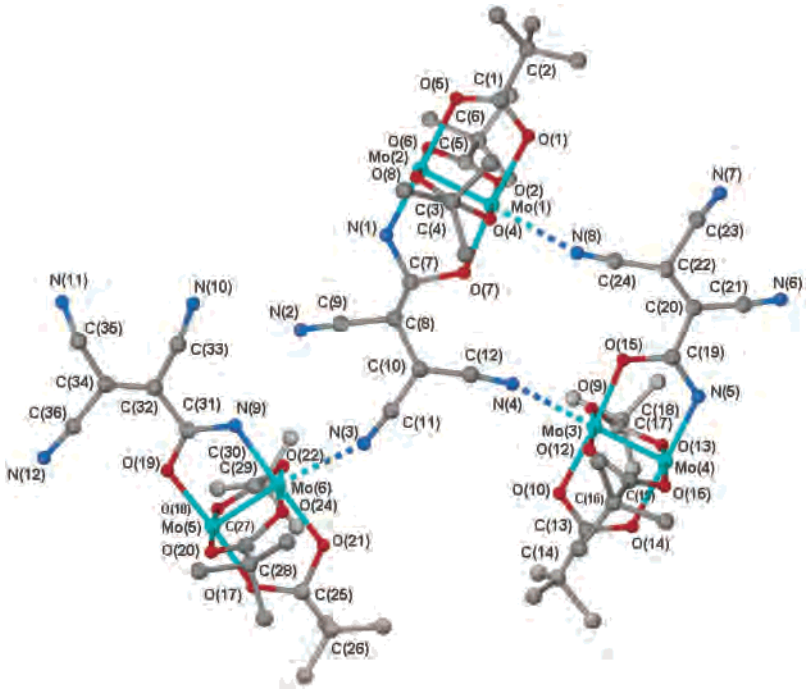

Figure 1. Ball and stick diagram of the asymmetric unit (excluding solvent molecules) in **2**. The asymmetric unit contains three $[Mo_2]$ units bridged by tricyanoacrylamide ligands.

Paratone-N and transferred at low temperature to a Siemens SMART 1K CCD platform diffractometer equipped with a low-temperature attachment operating at 133(2) K. A 16-h data set was collected to 0.74 Å resolution, using Mo Kα radiation. The data were corrected for absorption and decay with the program SADABS[12a] using a trigonal crystal system. Space group analysis and data sorting was performed with the program XPREP.[12b] The structure was solved and refined in the trigonal space group $P\bar{3}c1$ (No. 165) (Table 1). The structure was solved by direct methods with the SHELXTL program.[12a] All atoms in the $[Mo_2(O_2CCMe_3)_3((NC)_2CC(CN)CONH)]$ moieties were located from difference maps generated during subsequent refinement cycles. Refinement was carried out with a merohedral twinning matrix [0 −1 0 −1 0 0 0 0 −1], yielding a twinning ratio of 0.37961. In addition to 36 $[Mo_2(O_2CCMe_3)_3((NC)_2CC(CN)CONH)]$ moieties per cell, standard atomic volume analysis indicated that there are also 360 CH_2Cl_2 solvent molecules per cell. Of the 30 independent dichloromethane molecules, 13.5 could be located and refined with C−Cl and Cl−Cl bond restraints. These ordered dichloromethane molecules are all located between the infinite two-dimensional layers formed by the $[Mo_2(O_2CCMe_3)_3((NC)_2CC(CN)CONH)]_\infty$ units. The total volume of the void space and the approximate number of residual solvent electrons in the unit cell was calculated using the program PLATON.[12b] The solvent voids are large enough volume for approximately 16.5 more CH_2Cl_2 molecule for each formula unit. These solvent voids are infinite one-dimensional channels perpendicular to the $[Mo_2(O_2CCMe_3)_3((NC)_2CC(CN)CONH)]_\infty$ layers described above (Figure 2). Least-squares refinement and *tert*-butyl group and solvent disorder modeling were performed with the refinement program SHELXTL.[12a] Due to the solvent disorder, numerous crystallographic restraints were utilized.

(12) (a) SHELXTL: Sheldrick, G. M. BRUKER AXS, Madison, WI, 2001. SHELX97: Sheldrick, G. M. *Programs for Solving and Refining Crystal Structures*; University of Göttingen: Göttingen, Germany, 1997. (b) PLATON: Spek, A. L. *J. Appl. Crystallogr.* **2003**, *36*, 7. (c) X-Seed was used for molecular graphics: Barbour, L. J. *J. Supramol. Chem.* **2001**, *1*, 189.

Table 1. Crystal Data and Structure Refinement for $\{[Mo_2(O_2CCMe_3)_3(NC)_2CC(CN)CONH]\cdot 10CH_2Cl_2\}_\infty$ (**2**) and $\{[Mo_2(O_2CCMe_3)_3(NC)_2CC(CN)CONH]\cdot C_6H_6\}_\infty$ (**3**)

	2	**3**
empirical formula	$C_{93}H_{144}Cl_{60}Mo_6N_{12}O_{21}$	$C_{27}H_{34}Mo_2N_4O_7$
fw	4469.84	718.46
temperature	133(2) K	133(2) K
wavelength	0.71073 Å	0.71073 Å
crystal system	trigonal	monoclinic
space group	$P\bar{3}c1$	$C2/c$
unit cell dimens	$a = 46.976(2)$ Å	$a = 30.855(4)$ Å
	$b = 46.976(2)$ Å	$b = 11.1126(13)$ Å
	$c = 22.801(11)$ Å	$c = 17.964(2)$ Å
	$\alpha = 90°$	$\alpha = 90°$
	$\beta = 90°$	$\beta = 105.111(2)°$
	$\gamma = 120°$	$\gamma = 90°$
volume	43575.5(9) Å^3	5946.5(13) Å^3
Z	12	8
density (calcd)	2.044 Mg/m^3	1.605 Mg/m^3
abs coeff	1.67 mm^{-1}	0.893 mm^{-1}
$F(000)$	26712	2912
crystal size	0.46 × 0.40 × 0.20 mm^3	0.05 × 0.05 × 0.08 mm^3
reflns collected	113574	13804
refinement meth	full-matrix on F^2	full-matrix on F^2
data/restraints/params	26338/ 3392/ 1055	4999/59/262
GOF	1.020	1.026
R_1, wR_2 [F^2, $I > 2\sigma(I)$][a]	0.1581/0.3150	0.1000/0.1485

[a] $R_1 = \sum||F_o| - |F_c||/\sum|F_o|$, $wR_2 = \{\sum[w(F_o^2 - F_c^2)^2]/\sum[w(F_o^2)^2]\}^{1/2}$, goodness-of-fit $= S = \{[w(F_o^2 - F_c^2)^2]/(n-p)\}^{1/2}$, $w = 1/[\sigma^2(F_o^2) + (aP)^2 + bP]$.

Hydrogen atoms were fixed in idealized positions. Selected bond distances and angles are reported in Table 2.

$\{[Mo_2(O_2CCMe_3)_3((NC)_2CC(CN)CONH)]\cdot C_6H_6\}_\infty$, 3. A red hexagonal plate was selected and mounted on a Siemens SMART 1K CCD platform diffractometer. The intensities were corrected in the manner described for **2**. A total of 13804 reflections were measured at a maximum 2θ value of 49.4, of which 4999 were unique and 2226 were in the category of $I > 2\sigma(I)$ (Table 1). Symmetry related and multiply measured reflections were averaged

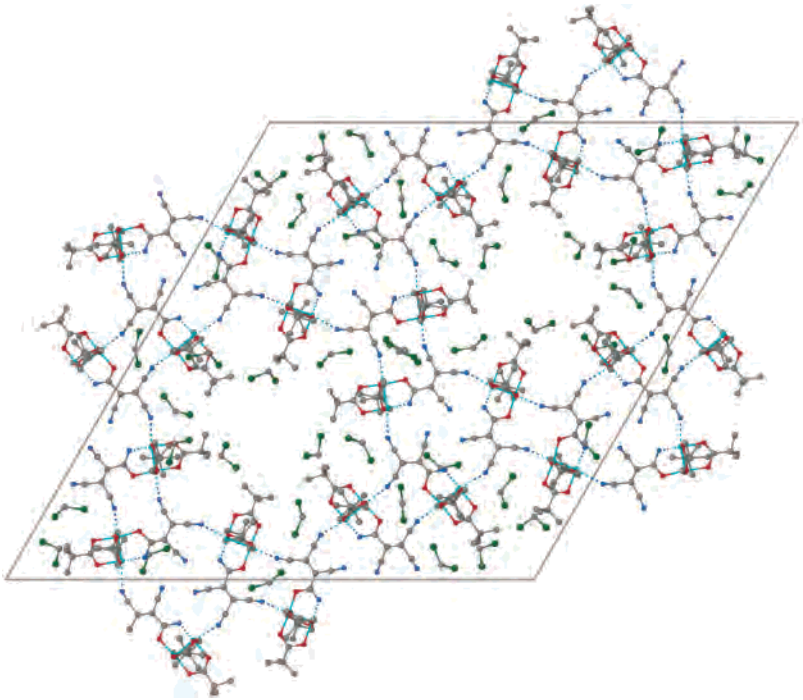

Figure 2. A projection of a single layer of the molecular packing of **2** in the *ab* plane. The Mo atoms and the axial Mo−N bonds display striking coplanar geometry and are almost exactly in the *ab* plane. For the sake of clarity several CH_2Cl_2 were removed, and the disorder is not depicted.

Table 2. Selected Bond Distances (Å) and Bond Angles (deg) for $\{[Mo_2(O_2CCMe_3)_3(NC)_2CC(CN)CONH]\cdot 10CH_2Cl_2\}_\infty$, **2**

Bond Distances

Mo(1)−Mo(2)	2.136(2)	Mo(2)−O(6)	2.093(13)	Mo(3)−O(12)	2.056(12)	Mo(4)−N(11)	2.615(15)	Mo(5)−N(12)	2.650(15)
Mo(1)−O(1)	2.136(13)	Mo(2)−O(8)	2.140(13)	Mo(3)−O(15)	2.026(12)	Mo(5)−Mo(6)	2.159(2)	Mo(6)−O(21)	2.169(12)
Mo(1)−O(2)	2.086(13)	Mo(2)−N(1)	2.029(14)	Mo(3)−N(4)	2.551(16)	Mo(5)−O(17)	2.067(12)	Mo(6)−O(22)	2.090(13)
Mo(1)−O(4)	2.113(13)	Mo(2)−N(7)	2.667(15)	Mo(4)−O(13)	2.151(13)	Mo(5)−O(18)	2.076(13)	Mo(6)−O(24)	2.098(13)
Mo(1)−O(7)	2.039(13)	Mo(3)−Mo(4)	2.146(2)	Mo(4)−O(14)	2.115(12)	Mo(5)−O(19)	2.025(13)	Mo(6)−N(9)	2.046(14)
Mo(1)−N(8)	2.543(15)	Mo(3)−O(9)	2.046(13)	Mo(4)−O(16)	2.049(12)	Mo(5)−O(20)	2.078(13)	Mo(6)−N(3)	2.584(16)
Mo(2)−O(5)	2.0153(12)	Mo(3)−O(10)	2.111(13)	Mo(4)−N(5)	2.066(15)				

Bond Angles

O(7)−Mo(1)−O(2)	94.9(5)	N(5)−Mo(4)−O(16)	93.5(6)	O(7)−Mo(1)−O(4)	93.9(5)	N(5)−Mo(4)−Mo(3)	88.0(4)
O(2)−Mo(1)−Mo(2)	90.0(4)	O(14)−Mo(4)−O(13)	84.6(5)	O(4)−Mo(1)−Mo(2)	91.8(4)	N(5)−Mo(4)−O(13)	93.9(5)
O(4)−Mo(1)−O(1)	84.5(4)	Mo(3)−Mo(4)−O(13)	90.9(4)	Mo(2)−Mo(1)−O(1)	90.9(4)	Mo(3)−Mo(4)−N(11)	171.2(4)
N(1)−Mo(2)−O(8)	99.7(6)	O(17)−Mo(5)−O(19)	174.5(5)	Mo(2)−Mo(1)−N(8)	176.3(4)	O(17)−Mo(5)−O(20)	86.7(5)
N(1)−Mo(2)−Mo(1)	91.2(5)	O(19)−Mo(5)−O(20)	91.7(4)	O(8)−Mo(2)−Mo(1)	90.4(5)	O(17)−Mo(5)−O(18)	86.0(6)
O(7)−Mo(1)−N(8)	82.4(5)	O(19)−Mo(5)−O(18)	95.4(5)	O(4)−Mo(1)−N(8)	89.6(5)	N(12)−Mo(5)−Mo(6)	177.3(4)
O(6)−Mo(2)−Mo(1)	91.1(5)	C(36)−N(12)−Mo(5)	164.1(5)	N(1)−Mo(2)−O(5)	176.9(5)	O(17)−Mo(5)−Mo(6)	92.6(5)
O(12)−Mo(3)−O(15)	93.8(5)	N(9)−Mo(6)−O(22)	93.1(5)	O(12)−Mo(3)−O(9)	173.8(5)	N(9)−Mo(6)−O(24)	95.6(5)
O(15)−Mo(3)−O(9)	90.7(5)	O(22)−Mo(6)−O(24)	170.8(5)	O(12)−Mo(3)−O(10)	87.8(5)	N(9)−Mo(6)−O(21)	179.0(5)
O(15)−Mo(3)−O(10)	176.7(5)	O(22)−Mo(6)−O(21)	85.9(4)	Mo(1)−Mo(2)−N(7)	169.8(3)	O(24)−Mo(6)−O(21)	85.5(4)
O(5)−Mo(2)−N(7)	79.4(4)	N(9)−Mo(6)−Mo(5)	89.0(4)	O(12)−Mo(3)−O(15)	93.8(5)	O(22)−Mo(6)−Mo(5)	89.0(3)

with the program XPREP.[12a] Systematic absences indicated that the crystal belongs to the space group *C*2/*c* (No. 15), with $R_{int} = 0.171$ and $R_\sigma = 0.221$. Structure solution was achieved from direct methods for all non-hydrogen atoms. Amide group disorder and the fully rotationally disordered *tert*-butyl group were modeled by refining the sum of conformations of the different disordered groups to be unity.

Results and Discussion

Syntheses. By stirring equimolar quantities of $Mo_2(O_2CCMe_3)_4$ and TCNE in either CH_2Cl_2 or CH_3CN under strictly anhydrous conditions (drybox atmosphere: $O_2 < 1$ ppm; $H_2O < 2$ ppm; reactants carefully dried at 30 °C under vacuum for a day and introduced directly into the reaction vessel inside the drybox) led to observation of no reaction. After the addition of 1 equiv of H_2O, however, an immediate color change ensued from yellow to dark green. After 1.5 h, highly air-sensitive, dark-red, hexagonal crystals were isolated. Elemental analyses as well as high-resolution mass spectrometry (high-resolution LSI-MS) established the formula to be $[Mo_2(O_2CCMe_3)_3((NC)_2CC(CN)CONH)]$, **1** (Scheme 1). In fact, the reaction was initially conducted under conventional anaerobic conditions in "dry" solvents, but trace quantities of water were suspected to lead to variable results. In order to explore the role of H_2O in this reaction, control experiments were conducted under strictly anhydrous conditions. These results indicate that, unexpectedly, H_2O is a prerequisite for the reaction, a fact that is supported by the finding that TCNE is hydrolyzed to the TC3A ligand with concomitant substitution of one pivalate bridge (Scheme 1).[13]

Scheme 1

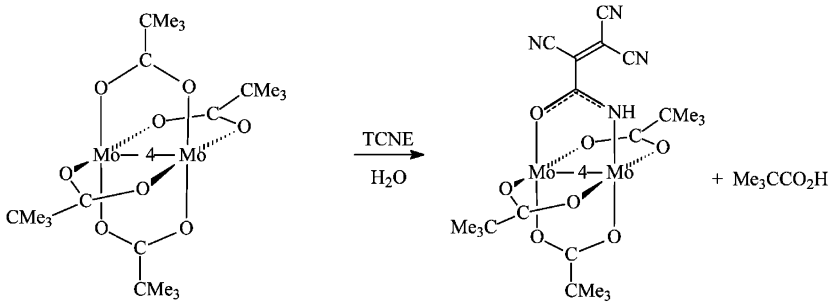

Spectroscopic Properties. On the basis of the redox chemistry of $Mo_2(O_2CCMe_3)_4$ and TCNE, one would expect compound **1** to be a charge-transfer complex of a metal-based radical of the type $Mo_2^{\bullet+}$ and a derivative of the $TCNE^{\bullet-}$ anion.[3] According to EPR measurements, however, **1** is diamagnetic with only a trace of residual paramagnetism. Moreover, the compound exhibits a well-resolved ^1H NMR spectrum in CD_3CN with two signals at +1.40 and +1.45 ppm in a 1:2 ratio, respectively. These signals are attributed to the methyl groups of three pivalate groups in two different magnetic environments. The ^{13}C NMR spectrum is in accord with this assignment, with three sets of two peaks in the ratio of 1:2 at 28.3 and 28.4, 41.7 and 41.8, and 195.9 and 197.2 ppm which are assigned to the primary, quaternary, and the carbonyl carbon atoms of the pivalate units. In addition, it is noteworthy that, as expected for the TC3A ligand, six resonances are present in the ^{13}C NMR spectrum (see Experimental Section) while a broad signal, characteristic of a labile −NH or −OH proton, is located at +11.75 ppm in the ^1H NMR spectrum. The infrared spectrum of **1** in the 1300−1500 cm^{-1} region is similar to that of the parent compound $Mo_2(O_2CCMe_3)_4$, an indication that the paddlewheel core has not been significantly altered in the course of the reaction. The solid-state IR spectrum of **1** revealed four ν(CN) bands at 2200, 2179, 2158, and 2149 cm^{-1} in accord with an unsymmetrically bonded polynitrile ligand. Two sharp features that appear at 3359 and 3336 cm^{-1} are assigned to the hydrolyzed TCNE ligand, TC3A.[11,13] The solution IR spectrum contains a sharp, intense ν(CN) band at 2204 cm^{-1}, with a weak shoulder appearing at 2219 cm^{-1}.[2,14,15]

Single-Crystal X-ray Crystal Structures. Two types of crystals suitable for X-ray diffraction were prepared from different crystallization procedures from samples of **1** (see Experimental Section). Both structures confirm the molecular structure proposed in Scheme 1. Red hexagonal-shaped crystals of $\{[Mo_2(O_2CCMe_3)_3((NC)_2CC(CN)CONH)]\cdot 10CH_2Cl_2\}_\infty$ (**2**) were grown from CH_2Cl_2, and dark red crystals of $\{[Mo_2(O_2CCMe_3)_3((NC)_2CC(CN)CONH)]\cdot C_6H_6\}_\infty$, (**3**) were obtained from C_6H_6.

Crystals of **2** were analyzed as belonging to the trigonal space group $P\bar{3}c1$ (No. 165) (Table 1) or the hexagonal space group *P*6*cc* (No. 184). Although the refinement was relatively poor due to twinning and considerable disorder, the data are of sufficient quality to allow for the important features of the structure to be ascertained.[16] Selected bond lengths and angles are listed in Table 2.

In compound **2**, the well-known paddlewheel structure of the $Mo_2(O_2CR)_4$ starting material is retained, but one of the original carboxylate groups has been substituted by a tricyanoacrylamidate ligand derived from TCNE (Figure 1). The modified TCNE ligands are coordinated to the Mo_2 unit in the axial positions to give a two-dimensional sheet structure wherein Mo_2 units are arranged in linked, pseudo-hexagonal rings through nitrile interactions to the modifed TCNE ligand (Figures 1 and 2). These sheets have hexagonal symmetry when projected along [001]. In addition to the axial N−Mo bonds (bond lengths from 2.543(15) to 2.667(15) Å), the Mo_2 units are linked by hydrogen bonds between the amide hydrogen and the nitrile nitrogen atoms. The existence of these hydrogen bonds confirms the assignment of the nitrogen and oxygen atoms in the amide groups. No suitable hydrogen bond acceptors were found in the vicinity of the oxygen atoms. The Mo−Mo vectors (bond lengths from 2.136(2) to 2.159(2) Å) are coplanar with the least-squares planes of the TC3A ligands. Interstitial CH_2Cl_2 molecules are located in the vacancies generated by two adjacent Mo_2 pairs in the rings; in addition there are numerous, highly disordered dichloromethane solvent molecules located near the 3-fold axes of the channels.

Crystals of **3** belong to the monoclinic space group *C*2/*c*. The asymmetric unit is depicted in Figure 3, and the structure

(13) Similar reactions were observed for addition of water to an acetonitrile ligand coordinated to quadruply bonded dimolybdenum complexes: (a) Cotton, F. A.; Daniels, L. M.; Haefner, S. C.; Kuhn, F. E. *Inorg. Chim. Acta* **1999**, *287*, 159. (b) Cotton, F. A.; Daniels, L. M.; Murillo, A.; Wang, X. *Polyhedron* **1998**, *17*, 2793.

(14) (a) Olbrich-Deussner, B.; Gross, R.; Kaim, W. *J. Organomet. Chem.* **1989**, *366*, 155. (b) Stufkens, D. J.; Snoeck, T. L.; Kaim, W.; Roth, T.; Olbrich-Deussner, B. *J. Organomet. Chem.* **1991**, *409*, 189.

(15) (a) Roth, T.; Kaim, W. *Inorg. Chem.* **1992**, *31*, 1930. (b) Olbrich-Deussner, B.; Kaim, W.; Gross-Lannert, R. *Inorg. Chem.* **1989**, *28*, 3113. (c) Kaim, W.; Olbrich-Deussner, B.; Roth, T. *Organometallics* **1991**, *10*, 410.

(16) The crystal structure for **2** is complex, with an extremely large unit cell (45000 $Å^3$). A large proportion (~57%) of this volume is occupied by solvent which is largely disordered. In these respects this structure has characteristics of a macromolecular protein-like structure for which an *R*-factor of 16% is understandable. In this case, it is mainly due to the large amount of solvent and disorder. All the possible twin laws were tested, and none gave better results than the one finally used. The data are good with a small *R*(int) value but, like proteins, the *R*-factor is larger than the *R*(int) value due to the large contribution of scattering by solvent which does not necessarily have a regular structure and contributes to diffuse scattering. The main point is that the molecular structure and connectivity of the atoms in the [Mo2X] units is irrefutable. An illustration is given in Figure S2 (see Supporting Information).

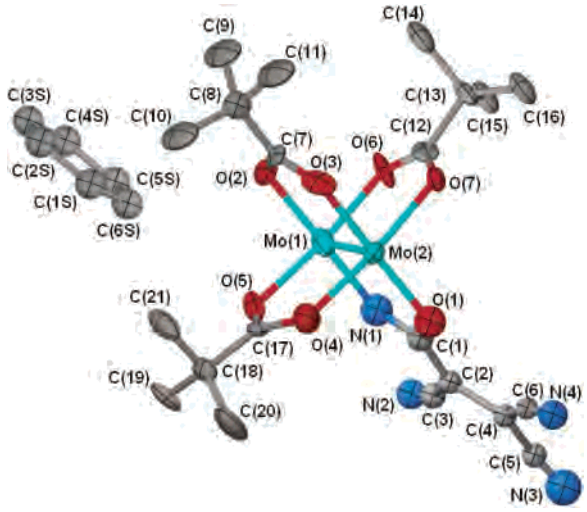

Figure 3. A thermal ellipsoid representation of the asymmetric unit in **3**. The disorder in the tricyanoacrylamide and *tert*-butyl groups as well as the benzene solvent molecule has been omitted for the sake of clarity.

consists of chains of a cyclic $[Mo_2]_2$ repeat pattern as shown in Figure 4. As in the case of **2**, the paddlewheel structure of the Mo_2 unit is retained, with three of the original carboxylate ligands as well as a TC3A ligand being coordinated via the O and N atoms of the amide group. In addition, two of the three CN groups are coordinated to the axial positions of two other equivalent Mo_2 units. The main difference in the structures of **3** and **2** is that in **3** the axial interactions involve the CN unit bound to the same C atom as the amide group and the trans 3-CN group rather than two 3,3′-CN groups. This difference leads to the formation of 1-D zigzag polymeric chains in which each Mo−Mo vector is nearly perpendicular to the acrylamide plane that connects the axial positions (Figure 4). The Mo−Mo bond length in **3** (2.1267(17) Å, Table 3) is longer than in the tetracetate dimolybdenum compound (2.093(1) Å).[17] It is also noteworthy that the Mo−O bond involving the TC3A ligand (2.056(9) Å) appears to be significantly shorter than those with the acetate ligands (from 2.083(8) to 2.113(9) Å), which hints at some degree of electronic delocalization from the ligand; this conclusion is supported by the shorter Mo−N bond length as well (2.039(10) Å). The Mo−N axial distances (2.561(10) and 2.577(10) Å) are much longer than the equatorial distance and are in the normal range for such distances. An interesting feature of the extended framework of **3** is the presence of bent nitrile groups as evidenced by the angles C6−N4−Mo1 = 121.8(8)° and C3−N2−Mo2 = 114.3(8)°. Previously characterized dimolybdenum compounds with polynitrile ligands exhibit angles for the M−NC interaction that are much closer to linearity, e.g., 160−170° as shown in Figure 2.[4c]

Finally, it is worth noting that, in both crystal structures **2** and **3**, the two *tert*-butyl groups above and below the acrylamide plane are bent away from the amide group as compared to the standard paddlewheel structure containing the same ligands. In addition, both structures exhibit disorder in the *tert*-butyl groups that are trans to the acrylamide ligand (Figure 1).

Electrochemistry. The electrochemistry of **1** is essentially the same in CH_3CN, PhCN, CH_2Cl_2, and THF. Typical cyclic voltammograms (CV) are shown in Figure 5 with the data

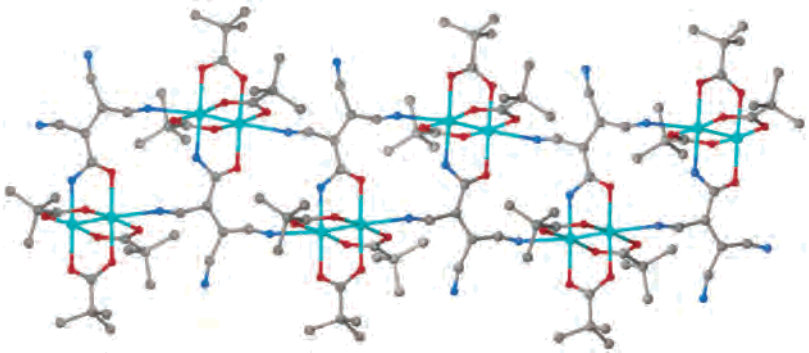

Figure 4. A portion of the infinite one-dimensional chain $\{[Mo_2(O_2CCMe_3)_3((NC)_2CC(CN)CONH)]\}_\infty$ of **3** emphasizing one of the 1-D chains along the *b* axis.

Table 3. Selected Bond Distances (Å) and Bond Angles (deg) for $\{[Mo_2(O_2CCMe_3)_3(NC)_2CC(CN)CONH]\cdot C_6H_6\}_\infty$, **3**[a]

Bond Distances

Mo(1)−N(1)	2.039(10)	Mo(2)−O(1)	2.056(9)	Mo(2)−N(2)#2	2.577(10)	Mo(1)−O(2)	2.091(8)	Mo(2)−O(3)	2.089(8)
Mo(1)−O(6)	2.087(8)	Mo(2)−O(7)	2.096(8)	Mo(1)−O(5)	2.083(8)	Mo(1)−N(4)#1	2.561(10)	Mo(2)−O(4)	2.113(9)
Mo(1)−Mo(2)	2.1267(17)								

Bond Angles

N(1)−Mo(1)−O(5)	93.1(3)	O(1)−Mo(2)−O(7)	93.6(3)	N(1)−Mo(1)−O(6)	92.5(4)	O(3)−Mo(2)−O(7)	86.3(3)
N(1)−Mo(1)−O(5)	93.1(3)	O(7)−Mo(2)−O(4)	172.3(3)	N(1)−Mo(1)−O(6)	92.5(4)	O(1)−Mo(2)−Mo(1)	91.1(3)
O(5)−Mo(1)−O(6)	173.7(3)	C(3)#2−N(2)#2−Mo(2)	114.3(8)	N(1)−Mo(1)−O(2)	177.6(4)	N(2)−Mo(2)−Mo(1)	91.6(3)
O(5)−Mo(1)−O(2)	86.7(3)	O(4)−Mo(2)−Mo(1)	91.2(2)	O(6)−Mo(1)−O(2)	87.6(3)	O(1)−Mo(2)−N(2)#2	91.3(4)
N(1)−Mo(1)−Mo(2)	90.8(3)	O(3)−Mo(2)−N(2)#2	86.5(4)	O(5)−Mo(1)−Mo(2)	92.3(3)	O(7)−Mo(2)−N(2)#2	91.9(3)
O(6)−Mo(1)−Mo(2)	90.6(2)	O(4)−Mo(2)−N(2)#2	85.1(3)	O(2)−Mo(1)−Mo(2)	91.6(3)	Mo(1)−Mo(2)−N(2)#2	175.7(3)
N(1)−Mo(1)−N(4)#1	86.5(4)	C(7)−O(3)−Mo(2)	117.2(8)	O(5)−Mo(1)−N(4)#1	98.6(3)	C(6)#2−N(4)#2−Mo(1)	121.8(8)
O(6)−Mo(1)−N(4)#1	78.8(3)	C(12)−O(6)−Mo(1)	118.7(9)	O(2)−Mo(1)−N(4)#1	91.2(4)	C(17)−O(4)−Mo(2)	116.0(8)
Mo(2)−Mo(1)−N(4)#1	168.9(3)	C(12)−O(7)−Mo(2)	116.6(9)	O(1)−Mo(2)−O(3)	177.7(4)	Mo(1)−Mo(2)−N(2)#2	175.7(3)

[a] Symmetry transformations used to generate equivalent atoms: #1 $-x + {}^1/_2, y - {}^1/_2, -z + {}^1/_2$; #2 $-x + {}^1/_2, y + {}^1/_2, -z + {}^1/_2$.

Table 4. Electrochemical Data for the Complex $[Mo_2(O_2CCMe_3)_3((NC)_2CC(CN)CONH)]$ **1**, and Its Precursors in Various Solvents with 0.1 M Bu_4NPF_6 at 1.5 mM Concentration at a Pt Electrode, 298 K [$E^{o\prime}$/V versus Ferrocene ($\Delta E_p = E_{pa} - E_{pc}$/mV)]

	2nd reduction		1st reduction		
	TC3A	TCNE	TC3A	TCNE	$[Mo^{III}\text{-}3.5\text{-}Mo^{II}]^{\bullet+}/[Mo^{II}\text{-}4\text{-}Mo^{II}]$
free TCNE					
CH_3CN		−1.20 (260)		−0.20 (60)	
PhCN		−1.20 (180)		−0.20 (90)	
CH_2Cl_2		−1.37 (340)		−0.17 (60)	
THF		−1.44 (200)		−0.30 (100)	
$[Mo_2(O_2CCMe_3)_4]$					
CH_3CN					−0.04 (70)
PhCN					−0.02 (60)
CH_2Cl_2					0.00 (180)
THF					−0.08 (100)
omplex **1**					
CH_3CN	−1.70[a]		−0.76 (90)		0.24 (60)
PhCN	−1.60[a]		−0.85 (80)		0.23 (60)
CH_2Cl_2	−1.70[a]		−0.84 (80)		0.28 (60)
THF	−1.85[a]		−1.00 (100)		0.22 (110)

[a] Irreversible peak potential.

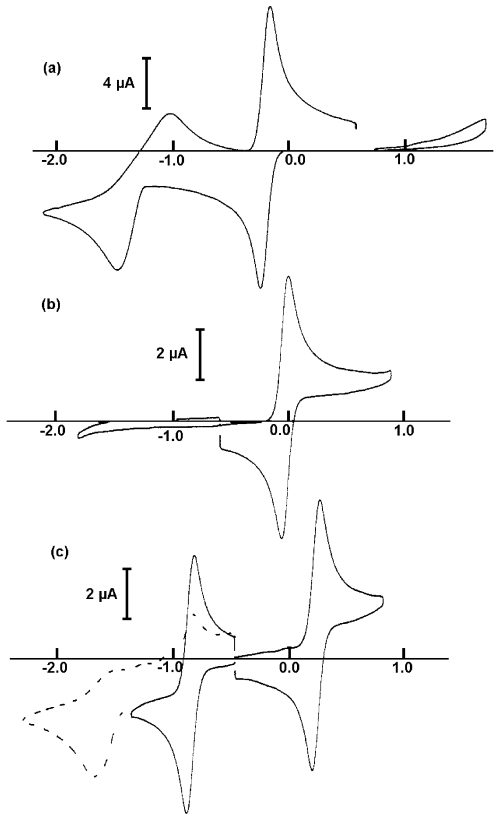

Figure 5. Comparative cyclic voltammetry of **1** and its precursors in PhCN, $[Bu_4N][PF_6]$ 0.1 M at a platinum electrode at $C = 1.5 \times 10^{-3}$ M: (a) free TCNE, (b) $Mo_2(O_2CCMe_3)_4$, and (c) complex **1** (the dashed line indicates a scan down to −2.2 V instead of −1.2 V, solid line).

being provided in Table 4. CV and rotating disk voltammetry (RDV, not shown) reveal the presence of a reversible one-electron oxidation process, and a reversible one-electron reduction process (in both cases $\Delta E_p = E_{pa} - E_{pc} \approx 60$ mV; $i_{pa}/i_{pc} \approx 1$). In addition, an irreversible process was also observed (Figure 5c). For the sake of comparison, the two successive reductions of free TCNE and the reversible oxidation of the parent compound $Mo_2(O_2CCMe_3)_4$ are provided in Figure 5a,b, respectively. It is interesting to note that, except for the redox potentials which are shifted, the electrochemistry of **1** resembles that of an independent organic acceptor derived from TCNE and the original $Mo_2(O_2CCMe_3)_4$ species. The CV peaks and RDV waves for the oxidation and first reduction of **1** exhibit essentially the same current intensities, an indication that these processes belong to a single species. It is also noteworthy that the CV peak and RDV wave intensities for **1** are very close to those observed for $Mo_2(O_2CCMe_3)_4$, which implies that the product has a similar diffusion coefficient D_0 and consequently the same nuclearity. The number of electrons exchanged for the two processes was confirmed by coulometry and found to be one electron. Bulk electrolysis of **1** at 0.5 V at a large surface electrode led to the isolation of the oxidation product of **1** which exhibits a reversible reduction at the same potential as the original oxidation process. The solution EPR spectrum of the oxidized species is typical of a delocalized mixed-valence dimolybdenum compound $[Mo^{III}-3.5-Mo^{II}]^{\bullet+}$ as shown in Figure 6, with $g = 1.939$, $A_{iso} = 25.5$ G.[8] Electrolysis at a potential for the first reduction step resulted in the decomposition of the complex.

The following conclusions can be drawn from the electrochemical study. In solution, compound **1** is a discrete entity that contains two electroactive fragments, namely, the [Mo-4-Mo] core and the acrylamide TC3A moiety. There is no indication that the TC3A is labile in any of the solvents that were used in these studies. Interestingly, the coordinated TC3A fragment retains the redox acceptor capability of TCNE, e.g., two reversible one-electron processes, but it is more difficult to reduce than TCNE. The most unusual finding, however, is that there appears to be no charge transfer, DA → $D^{\bullet+}A^{\bullet-}$, between the [Mo-4-Mo] and the TC3A bridge in the ground state. The HOMO level is clearly Mo−Mo based, and the LUMO level is TC3A-based. The difference between the oxidation and reduction potentials is generally considered to provide an evaluation of the HOMO/LUMO gap, at least comparatively.[8] In **1** the values obtained, $\Delta E^\circ = 1.00-1.22$ V (Table 4), suggest a large gap between the quadruply bonded Mo-4-Mo donor and the TC3A

(17) Cotton, F. A.; Mester, Z. C.; Webb, T. R. *Acta Crystallogr.* **1974**, *B30*, 2768.

Scheme 2

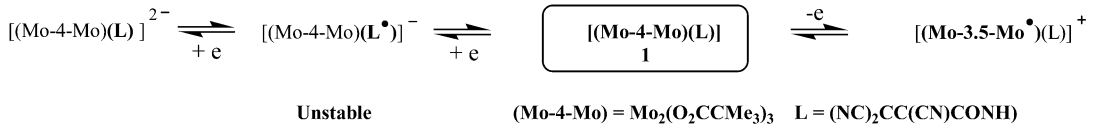

acceptor. This interpretation is supported by the results of the UV/vis/near-IR spectroscopy data.

As shown in Figure 7, the compound exhibits an intense, low-energy transition in the near-infrared region ($\lambda_{max} = 900$ nm, $\epsilon = 26000$ M^{-1} cm^{-1}) along with a broad feature at $\lambda_{max} \approx 400$ nm. On the basis of the electrochemistry, it is logical to assign the lowest electronic absorption transition to a metal-to-ligand charge transfer (MLCT) transition from a stabilized metal-based HOMO (ground state) to a π^* TC3A-based LUMO. The experimental HOMO/LUMO gap obtained from the electrochemical data, $\Delta E/V = E'^{o}_{ox} - E'^{o}_{red} \sim 1.1$ V, and from optical spectroscopy, $\Delta E = hc/\lambda \sim 1.4$ eV, are very similar.[18] These collective observations are in agreement with the redox pathways outlined in Scheme 2.

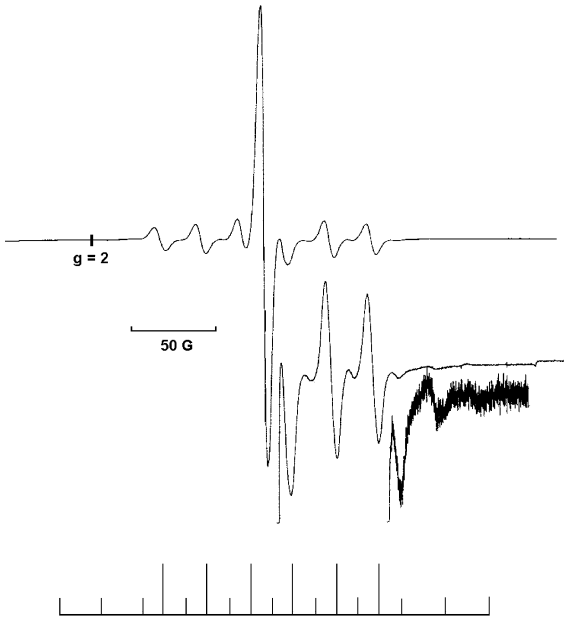

Figure 6. EPR spectrum of $\mathbf{1}^{\bullet+}$ generated by electrolysis in PhCN at 298 K showing the usual features of three components of one, six, and eleven lines expected for a delocalized electron on two molybdenum nuclei (^{92,94,96,98,100}Mo, $I = 0$, natural abundance ca. 75% and ^{95,97}Mo, $I = 5/2$, natural abundance ca. 25%).

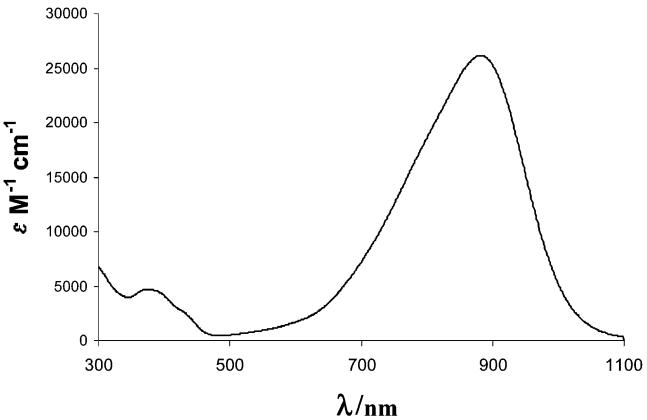

Figure 7. UV/vis/near-IR spectrum of **1** in CH_3CN.

Concluding Remarks

In this study, an unprecedented complex of the [Mo-4-Mo] variety has been characterized as a discrete species in solution as well as two different types of polymeric architectures in the solid state. Rather than observing a DA → $D^{\bullet+}A^{\bullet-}$ charge-transfer reaction, as one would predict from the redox chemistry of $Mo_2(O_2CCMe_3)_4$ and TCNE, we discovered that the reaction pathway involves the loss of a pivalate unit and an unusual type of TCNE hydrolysis to form the bridging tricyanoacrylamide anion TC3A. Although numerous TCNE hydrolysis reactions have been reported in the literature,[11,19] the most common route involves the release of an HCN molecule to form tricyanovinyl alcohol anion.[19] Of direct relevance to the present work is the fact that the addition product of H_2O and TCNE with no CN cleavage is a highly unusual hydrolysis route that has been reported to occur only under very high pressure and at elevated temperatures.[19] The structure of **1** from the reaction with $Mo_2(O_2CCMe_3)_4$ is apparently the only example wherein the hydrolysis of TCNE to give the tricyanoacrylamide anion has occurred under mild conditions.[13] The mechanistic pathway likely involves, as a first step, axial coordination of TCNE leading to $[Mo_2(O_2CCMe_3)_4{}^{\delta+}-TCNE^{\delta-}]$. Subsequent fixation of H_2O by the TCNE ligand and an acid−base equilibrium with one of the pivalate moieties are plausible steps in the hydrolysis of the nitrile. The subsequent coordination of the TC3A anion to Mo_2 would be the final step leading to **1**.

X-ray data collected on two different crystal forms of $[Mo_2(O_2CCMe_3)_3((NC)_2CC(CN)CONH)]$ clearly support the assignment of the solution structure as one that contains an acrylamide ligand in place of one of the pivalate groups in the paddlewheel structure. In the solid state, these units associate in two different architectures as illustrated by the connectivity patterns of the structures **2** and **3**. In structure **2**, the two bridging 3,3′-CN groups from the acrylamide are connected to two Mo_2 units. The angle between the two CN groups is about 120°; thus 2-D hexagonal rings are formed. In structure **3**, the two bridging 2,3-CN groups connected to two Mo_2 units are in trans positions, thereby leading to the formation of 1-D zigzag polymeric chains.

The spectroscopic and electrochemical properties of **1** in solution establish its formulation as a substitution product of an unoxidized Mo-4-Mo unit and an unreduced TC3A fragment. It is noteworthy that TC3A exhibits two accessible one-electron reduction processes similar to TCNE, but is harder to reduce, while the Mo-4-Mo unit is more difficult to oxidize in **1** than in $Mo_2(O_2CCMe_3)_4$. This complex can thus be described as an intimate complex of a donor and an

(18) Drago, R. S. *Physical Methods in Chemistry*; Saunders College Publishing: Philadelphia, 1977.
(19) Prince, M.; Hornyak, J. *J. Chem. Soc., Chem. Commun.* **1966**, 455.

acceptor, but with no charge transfer in the ground state, owing to the stabilization by a large HOMO/LUMO gap. Attempts to generalize this reaction to other tetracarboxylate derivatives of the same family $Mo_2(O_2CR)_4$ (R = Me, CH_2-CH_2CHMe_2, CF_3) and with alcohols instead of water are in progress. Efforts are also being made to understand the mechanistic process that leads to **1**, as it may be a general way to access new derivatives of interesting cyano acceptors with additional functionality.

Acknowledgment. This work was supported by the CNRS (UMR 6521) and Ministère de la Recherche. MR is acknowledged for a doctoral fellowship (B.L.G.). Prof. J.-Y. Saillard (U. de Rennes 1) and Dr. C. Gomez-Garcia (U. of Valencia) are thanked for helpful discussions. Dr. P. Jéhan, Prof. P. Guénot (CRMPO, Centre Régional de Mesures Physiques de l'Ouest, U. de Rennes 1), and Dr. R. Pichon and N. Kervarec (Service Commun de RMN, UBO) are thanked for recording of spectra and valuable discussions. K.R.D. thanks Michigan State University, Texas A&M University, and the National Science Foundation (CHE-9906583) for support.

Supporting Information Available: Projection of the molecular packing of **2** in the *ab* plane. Crystallographic data in CIF format. This material is available free of charge via the Internet at http://pubs.acs.org.

IC0351186